International Journal of Nanomedicine

Dovepress
open access to scientific and medical research

Open Access Full Text Article

ORIGINAL RESEARCH

Preparation and characterization of antiadhesion barrier film from hyaluronic acid-grafted electrospun poly(caprolactone) nanofibrous membranes for prevention of flexor tendon postoperative peritendinous adhesion

This article was published in the following Dove Press journal:
International Journal of Nanomedicine
22 August 2014
Number of times this article has been viewed

Shih-Hsien Chen[1]
Chih-Hao Chen[1,2]
KT Shalumon[1]
Jyh-Ping Chen[1,3]

[1]Department of Chemical and Materials Engineering, [2]Department of Plastic and Reconstructive Surgery, Chang Gung Memorial Hospital, College of Medicine, Chang Gung University, [3]Research Center for Industry of Human Ecology, Chang Gung University of Science and Technology, Taoyuan, Taiwan, Republic of China

Abstract: Peritendinous adhesion is one of the common complications encountered after tendon injury and subsequent surgery, and it can be minimized by introducing a physical barrier between the injured site and the surrounding tissue. An electrospun hyaluronic acid-grafted poly(caprolactone) (PCL-g-HA) nanofibrous membrane (NFM) is proposed as an alternative to current antiadhesion barrier films. HA is covalently grafted to surface-aminolyzed PCL nanofibers, using carbodiimide as the coupling agent. Pristine PCL and PCL-g-HA NFMs were characterized by scanning electron microscopy, thermogravimetric analysis, X-ray photoelectron spectroscopy, Fourier-transform infrared spectroscopy, and mechanical testing. In vitro cell culture with fibroblasts showed that PCL-g-HA NFMs reduced cellular adhesion on the membrane surface while maintaining cell proliferation. Animal experiments using a rabbit flexor digitorum profundus tendon model confirmed the efficacy of PCL-g-HA in reducing peritendinous adhesion, based on gross observation, histology, joint flexion-angle measurements, gliding tests, and biomechanical evaluation.

Keywords: peritendinous adhesion, hyaluronic acid, polycaprolactone, antiadhesion, nanofibrous membranes, barrier film, surface grafting

Introduction

Tissue adhesion occurs as a result of injury, foreign-body reaction, bleeding, or infection. Although adhesion is an important factor for wound healing, poor postoperative adhesion may result in pain, the need for a second surgery, and functional obstruction.[1] Following injuries to a flexor tendon, fibrotic adhesion will occur, making tendon repair complex and leading to limited postoperative gliding and range of the joint flexion.[2] Adhesions also worsen injuries related to flexor digitorum profundus (FDP) and flexor digitorum superficialis tendons in zone II of the hand.[3] Surgeons have used flexor-tendon autograft as a standard-care procedure for such tendon injuries, in addition to primary repair; however, postoperative adhesions still limit joint flexion or lead to joint contraction. The mechanisms underlying adhesion formation at injured or reconstructed sites are still unclear, but results suggest the arousal of intrinsic or extrinsic fibrosis, among other factors.[4]

Seprafilm® and SurgiWrap® are well-known antiadhesion barrier films approved by the US Food and Drug Administration for the prevention of peritendinous adhesions.

Correspondence: Jyh-Ping Chen
Department of Chemical and Materials Engineering, Chang Gung University, Kwei-San, Taoyuan, Taiwan 333, Republic of China
Tel +886 3 211 8800
Fax +886 3 211 8668
Email jpchen@mail.cgu.edu.tw

Chih-Hao Chen
Department of Plastic and Reconstructive Surgery, Chang Gung Memorial Hospital, College of Medicine, Chang Gung University, Kwei-San, Taoyuan, Taiwan 333, Republic of China
Tel +886 3 328 1200
Fax +886 3 328 9582
Email chihhaochen5027@yahoo.com.tw

submit your manuscript | www.dovepress.com
Dovepress
http://dx.doi.org/10.2147/IJN.S67931

Seprafilm is a dense hydrophilic film composed of sodium hyaluronate and carboxymethylcellulose.[5] The film can be used to detach or separate tissues surrounding a wound site during the middle phase of healing after abdominal surgery.[5] However, due to the longer healing time required after tendon surgery (more than 6 weeks) compared with that required after abdominal surgery, the use of Seprafilm in alleviating peritendinous adhesions is rather limited, considering its degradation period is only less than a week in vivo. SurgiWrap is an antiadhesion barrier film composed of polylactides.[6] Due to its hydrophilic characteristics and high density, SurgiWrap hinders exchanges of nutrients and wastes at the surgical site, which invariably lead to concerns regarding complications associated with tendon healing, considering the tendon has only limited blood circulation.

The protective membrane layer surrounding a tendon, which allows for movement, is the tendon sheath. The sheath is a membrane-like structure with two layers: an outer fibrotic layer and an inner synovial layer. The fibrotic layer forms condensations – pulleys – that act as fulcrums to aid tendon function, whereas the synovial layer secretes synovial fluid, which facilitates tendon gliding and tendon nutrition.[7,8] Hence, a biomimetic and biologically active tendon sheath should be able to effectively reduce peritendinous adhesion formation by not only acting as a cell-barrier layer but also allowing for tendon gliding at the membrane–tendon interface.

Poly(caprolactone) (PCL) is a good biodegradable polyester biomaterial for use in polymeric antiadhesion barrier films. PCL is a stable, low-cost, and readily available polymer with good mechanical properties.[9] However, due to its stiff nature and hydrophobicity, the applicability of PCL in antiadhesion products has been limited.[10] Hyaluronic acid (HA) is a natural polysaccharide with unique physicochemical properties, such as an outstanding lubricating capability, biocompatibility, and biodegradability.[11,12] HA is also the major component of the synovial fluid,[7] and is used extensively in antiadhesion barrier films for abdominal surgery.[5] To imitate the function of a tendon sheath, HA could be used as the major component in a barrier film to impart a lubricating effect, which should help mimic the function of the inner synovial layer and may also cooperatively block fibroblast attachment and cell penetration from the outer layer. Indeed, previous reports have indicated that membranes made from HA can prevent peritendinous adhesions when used as physical barriers.[13]

Electrospinning (ES) is a versatile method for the preparation of fibers from natural and synthetic polymers with dimensions ranging from a few nanometers to several micrometers. During the ES process, random nanofibers form on a grounded collector when a polymer solution is pushed out from a needle at a constant rate under a high applied voltage.[14] Considering their small pore size and high porosity, the application of electrospun nanofibrous membranes (NFMs) as an antiadhesion barrier may be warranted by preventing fibroblast penetration from surrounding tissues, which are responsible for adhesion formation, without hindering the transport of nutrients and wastes.

Various reports explaining the antiadhesion barrier properties of electrospun NFMs made from PCL, poly(lactide-*co*-glycolide), polylactide-poly(ethylene glycol) triblock copolymer, and a chitosan/alginate blend have been published.[9,15–18] These NFMs were only tested in abdominal antiadhesion animal models rather than for preventing peritendinous adhesion. A recent report suggests the use of NFMs consisting of a core–sheath nanofiber with an HA microgel inner core and a PCL outer-shell layer for the antiadhesion of repaired tendons.[19] However, maintaining the long-term lubrication effect of HA may be difficult in this NFM-based antiadhesion barrier. A second report details the preparation of electrospun ibuprofen-loaded poly(l-lactic acid)-polyethylene glycol diblock copolymer NFM for the prevention of peritendinous adhesions.[20] Indeed, NFMs made from polymer blends or copolymers are expected to enhance the antiadhesion function of a single-component homopolymer NFM. However, in this case, extreme care is required in controlling the ES conditions, and complex copolymerization steps must be followed. One of the alternatives to using copolymers or polymer blends in ES is to prepare a surface-grafted NFM by grafting bioactive macromolecules to a nanofiber surface. Compared to fabricating nanofibers from polymer blends, surface-grafting macromolecules to a single-component nanofiber after the ES step may allow for more flexibility in choosing the grafted macromolecule and the ES condition than preparing a composite NFM.[21]

Taking advantage of good mechanical properties and intrinsic antiadhesion properties, we propose that a PCL NFM grafted with HA would improve peritendinous antiadhesion performance. Our primary objective in this study was to prepare and characterize electrospun PCL and HA-grafted PCL (PCL-g-HA) NFMs. Using the combined advantages of the material's nanofibrous structure and properties in film form, we also demonstrated the effect of HA grafting on the improved efficacy of PCL-g-HA over PCL NFM and Seprafilm in preventing peritendinous adhesions in vivo.

Materials and methods

Materials

HA with a mean molecular weight of 1.3×10^6 Da was provided by Shandong Freda Biochem. PCL (average molecular weight 80,000 Da), 2-(*N*-morpholino)ethanesulfonic acid (MES), 1-ethyl-3-(3-dimethylaminopropyl) carbodiimide hydrochloride (EDC), *N*-hydroxysuccinimide (NHS), antibiotics, and trypsin–ethylenediaminetetraacetic acid were purchased from Sigma-Aldrich. CellTiter 96® AQueous One solution was obtained from Promega. Dulbecco's Modified Eagle's Medium and fetal bovine serum were purchased from Sigma-Aldrich and HyClone, respectively. Rhodamine–phalloidin and 4′,6-diamidino-2-phenylindole (DAPI) solutions for cell staining were obtained from Thermo Fisher Scientific.

Preparation of electrospun PCL NFM

A PCL solution (12 wt%) was prepared in a methylene chloride/*N*,*N*'-dimethylformamide (weight ratio 4:1) mixed-solvent system. NFM was prepared at room temperature using a 23-gauge stainless steel needle fitted to a glass syringe containing 20 mL polymer solution and a syringe pump (KD Scientific) operated at 1.0 mL/h. A potential of 20 kV was generated by a high-voltage power supply (Glassman) by fixing the needle tip-to-target distance at 15 cm. Aluminum foil was used as the grounded metallic stationary target. The thickness of the NFM was 200±50 μm.

Surface modification of PCL NFM

An aminolyzed PCL NFM (PCL-NH_2) with active surface-amine groups was first prepared by reacting the PCL NFM (8×6 cm) with 10 wt% 1,6-hexanediamine in 200 mL isopropanol for 8 hours.[22–24] Following aminolysis, the membrane was washed in distilled deionized (DDI) water and dried under vacuum. A 200 mL HA solution (10 mg/mL) was prepared in 0.05 M MES buffer (pH 5.0). EDC and NHS were added to the HA solution to reach a final EDC concentration of 10 mg/mL and an EDC:NHS molar ratio of 0.6. The PCL-NH_2 NFM was immersed in the HA solution immediately and maintained overnight, followed by washing with copious amounts of distilled water.

Characterization of NFM

The NFM morphology was observed using scanning electron microscopy (Hitachi S3000N). At least 100 random fibers observed in ten images were selected to measure the fiber diameters using the ImageJ software program. Capillary flow porosimetry (PMI CFP-1100-AI; Porous Materials) was used to measure the pore size of the NFM using a 21 dyn/cm surface-tension wetting agent. Spectroscopic characterization for chemical analysis was performed using a Horiba FT-730 Fourier-transform infrared spectrometer over a wavenumber range of 600–4,000 cm^{-1} at a resolution of 2 cm^{-1}. A Physical Electronics PHI 1,600 ESCA photoelectron spectrometer equipped with a multichannel detector and a spherical capacitor analyzer was used to perform X-ray photoelectron spectroscopy (XPS). The X-ray source was a magnesium anode operated at 15 kV and 400 W, and the pressure in the analysis chamber was maintained at 2×10^{-6} Pa. The thermal properties of the NFMs were evaluated using thermogravimetric analysis (TGA) (TGA 2050; TA Instruments) from 25°C to 700°C at a heating rate of 10°C/min. The tensile properties of the materials were determined using a material-testing machine (Tinius Olsen H1KT) with a 10 N load cell. Test samples were cut into dimensions of 1 cm ×5 cm ×200 μm and were vertically mounted on two mechanical gripping units by leaving a 3 cm gauge length for mechanical loading. Data were recorded at a deforming rate of 5 mm/min. The ultimate tensile strength, elongation at break, and Young's modulus were obtained from stress-strain curves.[25]

The equilibrium water contents of PCL and PCL-g-HA NFMs were determined from disk-shaped NFM samples (200 μm in thickness ×14 mm in diameter) immersed in 20 mL DDI water at 25°C. The wet weight of the NFM was recorded periodically, and the water uptake (%) was calculated using the following equation:

$$\text{Water uptake (\%)} = \left[\frac{w_t - w_o}{w_o}\right]\times 100, \qquad (1)$$

where w_t is the weight of the wet membrane measured at 24 hours, and w_o is the weight of the dry membrane measured at time 0. The wettability of the NFM surface was determined by a contact-angle analysis system (First Ten Ångstroms) using DDI water. The contact angles were measured after 5 seconds at 25°C and calculated using an automated fitting program (FTA-125). Each value reported was the average of three measurements for three replicate NFM samples.

In vitro cell culture

NFMs were prepared as disks (1.4 cm in diameter), sterilized with 75% ethanol overnight in 24-well cell culture plates and rinsed three times with phosphate-buffered saline (PBS) before use. Human foreskin fibroblast (Hs68) cells (American Type Culture Collection CRL-11372) at passage numbers 4–6 were used. Each well containing a

prewet membrane in the culture plate was seeded with a 0.1 mL aliquot of cell suspension (1×10^5 cells/mL) and incubated at 37°C for 4 hours to allow for cell adhesion. The membrane was transferred to a new well containing 1 mL culture medium (Dulbecco's Modified Eagle's Medium supplemented with 10 vol% fetal bovine serum and 1 vol% antibiotic–antimycotic). The 3-(4,5-dimethylthiazol-2-yl)-5-(3-carboxymethoxyphenyl)-2-(4-sulfophenyl)-2H-tetrazolium assay using the CellTiter 96 AQueous One solution was used to measure the viable cell number after 1 and 7 days. An enzyme-linked immunosorbent assay plate reader (BioTek Synergy HT) was used for the colorimetric measurements of the formazan product at 492 nm. F-actin staining was used to observe the cytoskeletal arrangements of attached Hs68 cells on the membrane after 24 hours. The membrane was washed twice with PBS, followed by fixing in 4% paraformaldehyde for 10 minutes. After the fixative was eliminated, cells were washed repeatedly in PBS and permeabilized with 0.1% Triton X-100 in PBS for 10 minutes. Then, samples were washed twice in PBS and stained with 20 μg/mL of rhodamine–phalloidin solution for 30 minutes. Before being imaged under a confocal laser scanning microscope (Zeiss LSM 510 Meta), samples were washed twice in PBS, and cell nuclei were stained with 1 μg/mL DAPI for 5 minutes. The excitation and emission wavelengths for rhodamine–phalloidin are 540 and 573 nm, respectively, and the corresponding wavelengths for DAPI are 340 and 488 nm.

Animal study

Sixty-four 3-month-old male New Zealand White rabbits (National Laboratory of Animal Breeding and Research Center, Taiwan, People's Republic of China) weighing 2.5–3.0 kg were used in this study. The guidelines of the Institutional Animal Care and Use Committee of Chang Gung University were followed in all animal experiments. Due to its similarity to the flexor mechanism of human digits, a rabbit FDP tendon model was used in the experiment. The rabbits were preanesthetized by the intramuscular injection of ketamine (20 mg/kg). Before surgery, the hind paws of the rabbits were shaved and prepared. General anesthesia was then induced by applying 4% isoflurane using a mask and maintained by the administration of 2% isoflurane with O_2 at 2.5 L/min. The surgical field was sterilized with iodine solutions; the nonsterile area was covered with sterile drapes. All surgical instruments were sterilized and kept sterile throughout the entire procedure.[26] Through a 2.0 cm longitudinal incision at the proximal phalanx of the second and third digits of the hind paws, the zone II flexor tendons were released from the tendon sheaths. After the removal of flexor digitorum superficialis tendons, the FDP tendons were completely divided just distally to the chiasm and proximally to the vincula, and were then repaired by the modified Kessler core-suture technique using 5-0 polydioxanone sutures (Ethicon). One of four different treatments, one control and three experimental, was applied randomly to each tendon of the animal model. In the experimental group, an 8×10 mm piece of Seprafilm, PCL NFM, or PCL-g-HA NFM was used to wrap the repair site of the FDP tendon, whereas PBS was applied in the control group. After operation, the skins were closed with 4-0 Ethicon sutures, and 3 mg/kg gentamicin was administered intramuscularly as a prophylactic antibiotic. The wounds were sterilized and dressed with gentamicin ointment to prevent infection. The hind limb was immobilized in a weight-bearing cast.

The killing of animals was arranged at 2 and 8 weeks after surgery with lethal doses of pentobarbital (0.5 g/kg body weight). The feet were transected at the ankle joint, and the second and third toes were assigned randomly for the evaluation of peritendinous adhesions. The measurements included gross and histological analysis and measurements of the range of motion (flexion angles) of the distal interphalangeal (DIP) and proximal interphalangeal (PIP) joints, tendon gliding excursion, and the maximum force needed to pull the tendon out of the tendon sheath. Postoperative mechanical testing was also performed to examine the breaking strength of the healed tendon after 2 weeks.

Gross and histological evaluation

The second and third toes of each foot were retrieved and opened for gross evaluation of adhesion after removing the skin sutures along the original incisions.[27] The severity and extent of peritendinous adhesion were recorded. For histological examination, 10% formaldehyde in PBS was used to fix the second and third toes of the rabbits. Samples were sectioned into 4 μm slices, and hematoxylin and eosin staining was used according to standard protocols. The inflammatory reaction and peritendinous adhesion formation were evaluated at 2 and 8 weeks postoperation.

Range-of-motion and gliding tests

Range-of-motion analysis was conducted using a custom-made apparatus. The FDP tendon was transected at the proximal metacarpal level and sutured to a cable connected to a load transducer in a custom-made range-of-motion apparatus. The metacarpophalangeal joint was fixed by inserting a

wire longitudinally through the metacarpal and the proximal phalanx. Two reflective markers of T-shaped pins were used to fix the proximal, middle, and distal phalanges. A nonslip clamp was used to avoid slipping while the prepared digit was mounted on the range-of-motion apparatus. To ensure full extension of the digit, a 50 g weight was attached to the extensor tendon. Angular range of motion was created by pulling the tendon using an actuator at a rate of 3 mm/s. This pulling caused digital flexion (angular motion), and the angle measured between the distal phalanx and the middle phalanx determined the DIP joint flexion. The angle between the middle phalanx and the proximal phalanx determined the PIP joint flexion.[12]

Two metal pins were used for functional evaluation based on tendon gliding displacement. We used the proximal phalanx to fix digits to a table and applied traction to the tendon to measure the flexion of the three distal joints. After removing skin, subcutaneous tissue, and other flexor tendons, the FDP tendon was exposed. The tendon sheath and FDP tendon were marked at the exit from the sheath. A fixed counterweight from the distal phalanx was applied to elongate the interphalangeal joints fully. By applying a 1 N force, the FDP tendon was pulled out of the sheath tunnel, and the distance after pulling was measured with a micrometer caliper. The gliding excursion of the FDP tendon was considered the distance of tendon gliding.[28]

Biomechanical analysis

A material-testing machine (Tinius Olsen H1KT) with a 50 N load cell was used to evaluate the extent of peritendinous adhesion by pullout-force measurements.[28] The pulling rate of FDP tendon was 5 mm/min, and the displacement and the load (N) were recorded. The pullout force (N) was defined as the maximum force necessary to pull the tendon out of the tendon sheath. Tendon healing was further evaluated by testing the mechanical strength of healed tendons at 2 weeks postoperation. To this end, the Tinius Olsen H1KT with a 50 N load cell was used in combination with nonslip clamps (HT-51). After the distal and proximal ends of the repaired FDP tendon were fixed, the tendon was pulled uniaxially at 5 mm/min to rupture. The maximum tension force was recorded as the breaking force of the healed tendon.

Statistical analysis

All data were expressed as means ± standard deviations. A Wilcoxon rank-sum test (paired comparison) was used for statistical analysis, with a *P*-value less than 0.05 considered statistically significant.

Results and discussion

Characterization of PCL and PCL-g-HA NFMs

The ES process produces bead-free and continuous PCL nanofibers (Figure 1A), and also preserves the nanofiber morphology after the chemical grafting of HA (Figure 1B). The histograms reveal that the average fiber diameter of PCL NFM increased from 432.1 to 673.1 nm after HA grafting (Figure 1, C and D); however, there was no statistical difference among the values (Table 1). The pore-size distribution of the membranes shifted from 0.2–2.5 to 0.2–3.3 μm, with the mode of the pore size increasing from 1.0–1.1 to 1.7–1.8 μm after HA grafting (Figure 1, E and F). This shift caused a significant increase in average pore size from 1.17 (PCL NFM) to 1.93 μm (PCL-g-HA NFM) (Table 1). The increases in fiber diameter and pore size might have stemmed from the space occupied by and the electrostatic repulsion from the surface-grafted HA molecules, respectively. The surface properties of NFMs were expected to be affected by the presence of HA, which was determined by water contact-angle measurements, as shown in the inserts of Figure 1, A and B. Because PCL is hydrophobic, the pristine PCL NFM showed a contact angle of 117.8°, whereas the HA-grafted NFM (PCL-g-HA) showed a drastic decrease in contact angle to 95.6° (Table 1). Undoubtedly, this reduction was due to the presence of hydrophilic HA molecules on the PCL nanofiber surface.

The TGA curves and the first derivative of the TGA (DTG) curves were used to analyze the thermal properties of the NFMs (Figure 2, A and B). The TGA curves indicate a large weight loss between 200°C and 500°C for all samples, due to the thermal decomposition of HA and PCL. For HA, the initial weight loss from 60°C to 100°C represents the evaporation of residually bound water from HA. Another thermal decomposition event occurred starting at –200°C, with the maximum weight loss observed at 231°C, which gave rise to a residual weight of 31.0%.[29] The onset of weight loss for the PCL NFM started at approximately 350°C, with the peak decomposition temperature occurring at 407°C.[30] For the PCL-g-HA NFM, the weight loss started at –200°C, with a broad peak at 214°C and a sharp peak at 395°C in the DTG curve. The former peak corresponds to HA, and the latter to PCL.[29,30] The higher residual mass of PCL-g-HA NFM (4.0 wt%) compared with that of PCL NFM (1.4 wt%) at 500°C could be correlated with the weight of grafted HA in the PCL-g-HA NFM. Figure 2C shows the Fourier-transform infrared spectra of different NFMs extracted between 2,000 and 600 cm^{-1}. The major peaks in the spectra of both the PCL and PCL-g-HA NFMs are attributed

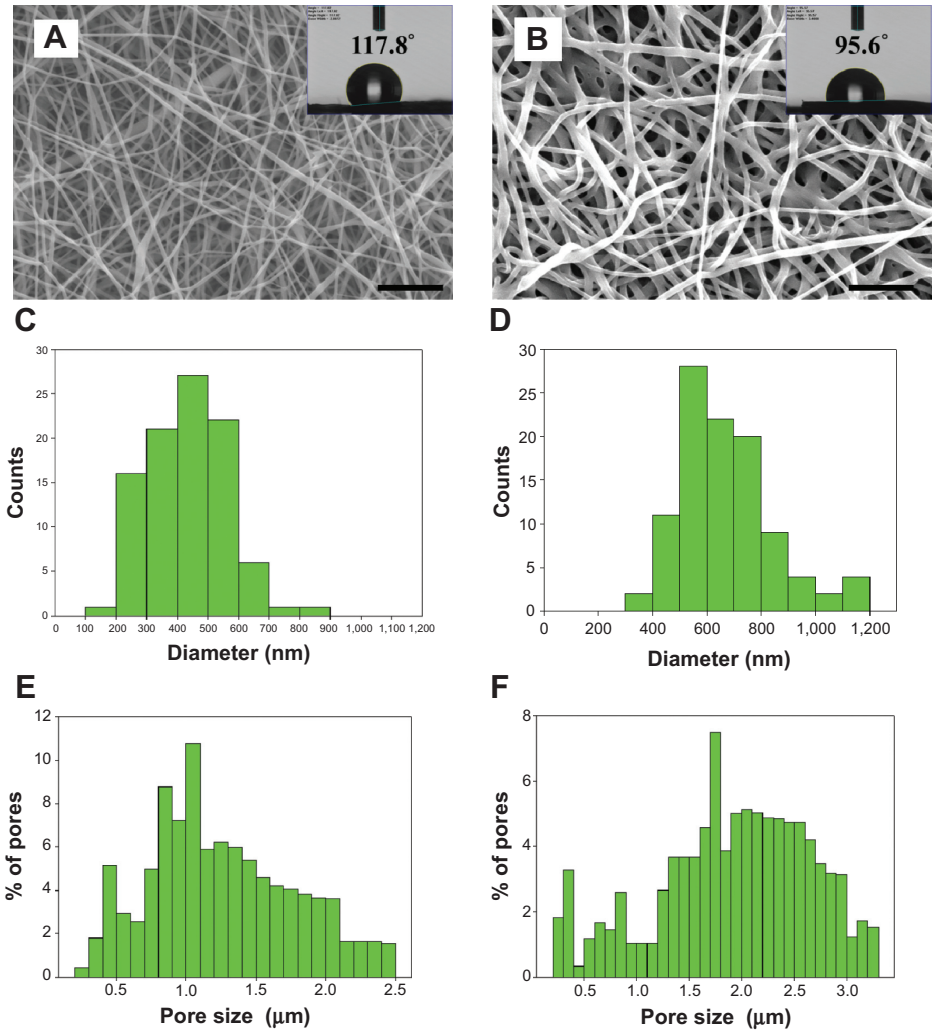

Figure 1 Scanning electron micrographs (bar =10 μm) (**A**, **B**), fiber-diameter distribution (**C**, **D**), and pore-size distribution (**E**, **F**) of electrospun PCL (**A**, **C**, **E**) and PCL-g-HA (**B**, **D**, **F**) nanofibrous membranes. The inserts in (**A**) and (**B**) show the water contact-angle measurements of the membranes.
Abbreviation: PCL-g-HA, hyaluronic acid-grafted poly(caprolactone).

to the ester stretching of PCL at 1,726 cm^{-1}.[22] The stretching bands of amide I and II at 1,616 and 1,564 cm^{-1} are only observed for the PCL-g-HA NFM, suggesting the presence of HA on the surface of PCL-g-HA nanofibers.[22]

Surface characterization was performed using XPS. The survey-scan spectra and the high-resolution C_{1s} peaks of the PCL and PCL-g-HA NFMs are shown in Figure 3. Two separated peaks corresponding to C_{1s} (286 eV) and O_{1s} (534 eV) are shown in all XPS spectra (Figure 3A). A distinct N_{1s} peak at 401 eV is observed in the spectra of the aminolyzed ($PCL-NH_2$) and PCL-g-HA NFMs (Figure 3A), confirming the successful introduction of NH_2 groups into the PCL-fiber surface. The nitrogen surface concentration increased from 0.74% to 2.68% after HA grafting (Table 2), with additional nitrogen present in the *N*-acetyl glucosamine subunit of HA. The presence of HA was further detected based on a distinct Na_{1s} peak at 1,073 eV observed only in the spectrum of the PCL-g-HA NFM (Figure 3A), with sodium ions present in HA sodium salts. The fractions of different carbon functional groups were calculated from high-resolution XPS C_{1s} spectra (Figure 3, B–D) and are reported in Table 3. The three peaks at 286.6, 288.1, and 290.6 eV were assigned to the C–C, C–O, and O=C–O bonds, respectively, in the

Table 1 Fiber diameter, pore size, and water-contact angle of nanofibrous membranes

Membrane	Fiber diameter (nm)	Pore size (μm)	Contact angle (degrees)
PCL	432.1±123.4	1.17±0.01	117.8±4.1
PCL-g-HA	673.1±172.7	1.93±0.06*	95.6±0.4*

Note: *$P<0.05$ compared with PCL.
Abbreviations: PCL-g-HA, hyaluronic acid-grafted poly(caprolactone); PCL, poly(caprolactone).

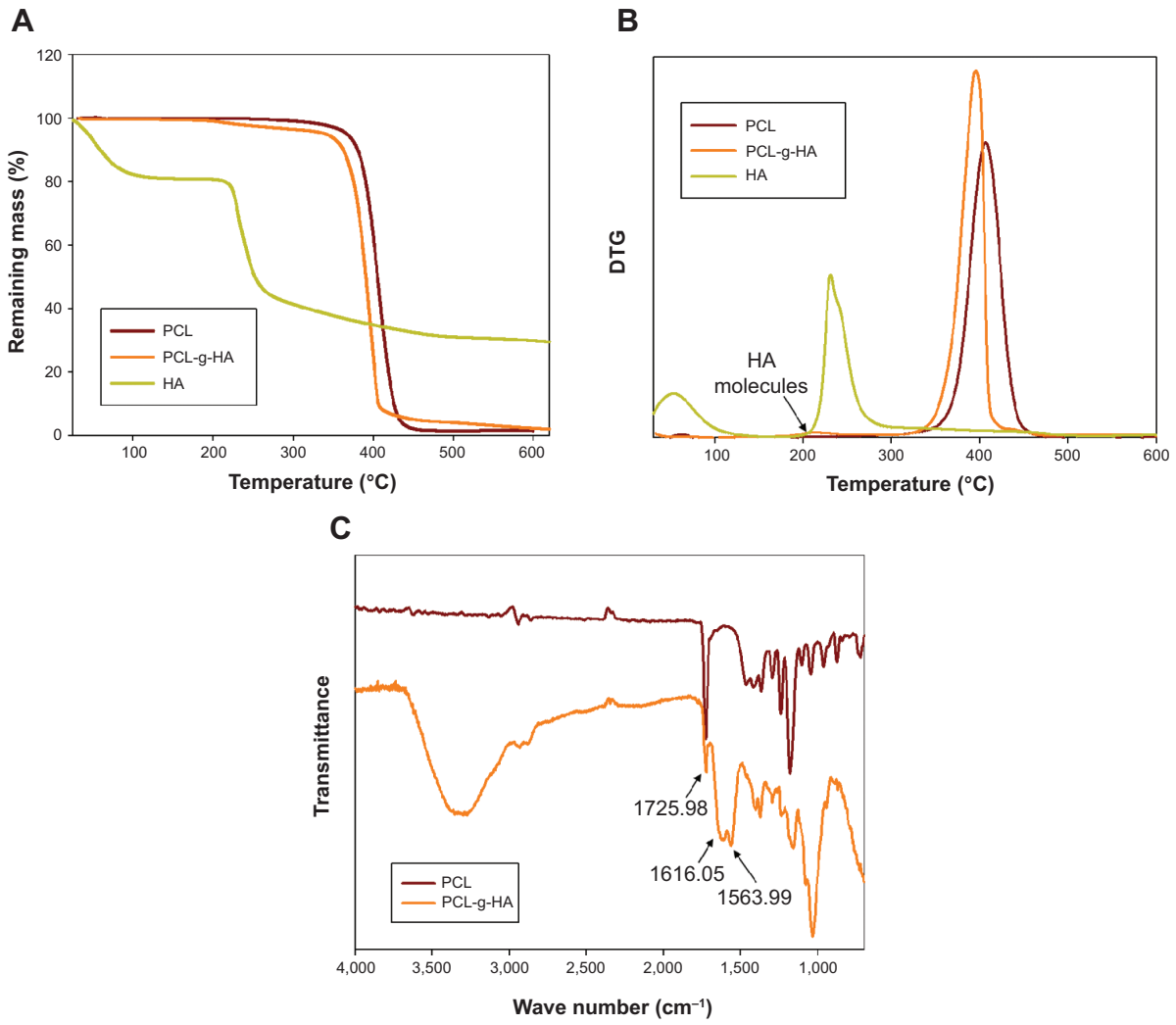

Figure 2 Thermogravimetric analysis (TGA) (**A**) and first derivative of TGA (DTG) curves (**B**) and Fourier-transform infrared spectroscopy spectra (**C**) of PCL and PCL-g-HA nanofibrous membranes.
Abbreviations: PCL-g-HA, hyaluronic acid-grafted poly(caprolactone); PCL, poly(caprolactone).

PCL polymer chain. The C_{1s} spectrum revealed a new peak at 289.3 eV for PCL-NH_2, due to the reaction between the NH_2 groups of the diamine with the –COO– ester group of PCL to form NH–C=O after aminolysis. An increase in the NH–C=O peak fraction from 7.77% to 11.20% was observed for the PCL-g-HA NFM, due to the contribution of amide carbons in HA or the newly formed amide bonds between PCL-NH_2 and HA.[10,24,31]

The water absorptivities of the NFMs are compared and shown in Figure 4A. As expected, the PCL NFM exhibited relatively low water sorption due to its hydrophilic nature. The water uptake of the PCL NFM increased 11.8-fold from 2.6% to 30.6% with the grafting of highly water-absorptive HA molecules. The water-absorptive swelling of the PCL-g-HA NFM is expected to impart a hydrogel-like nature to the membrane surface and promote interfacial gliding at the membrane-tendon interface, which is similar to the function of the synovial fluid secreted from the tendon sheath.[17] The stress–strain behaviors of the NFMs were measured, and typical stress–strain curves are reported in Figure 4B. The HA surface grafting enhanced the elongation at break by 87% (Table 4). With regard to the ultimate tensile stress and Young's modulus, the PCL-g-HA NFM also showed significantly higher values (1.21 and 1.12 times) than the PCL NFM (Table 4). Because there was no significant increase in fiber diameter after HA grafting (Table 1), the increase in tensile stress and Young's modulus could be ascribed to the covalent binding of HA molecules to the PCL-fiber surface.[32] The better mechanical performance in terms of higher stretching capability and breaking strength will undoubtedly facilitate the application of PCL-g-HA NFMs to the limited and highly curved space around a repaired tendon after surgery.

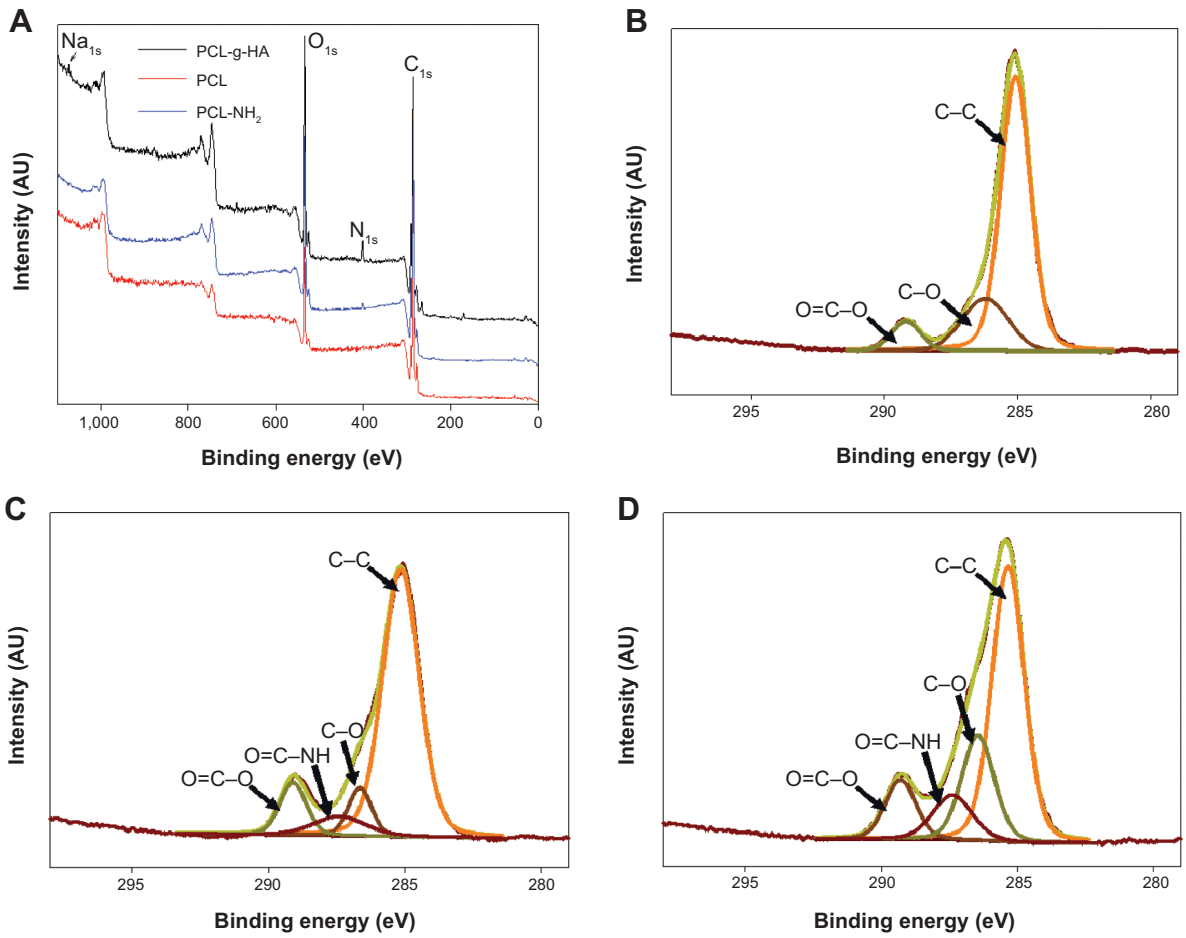

Figure 3 X-ray photoelectron spectroscopy survey-scan spectra (**A**) and C_{1s} spectra of PCL (**B**), aminolyzed PCL (PCL-NH_2) (**C**), and PCL-g-HA (**D**) nanofibrous membranes.

Abbreviations: PCL-g-HA, hyaluronic acid-grafted poly(caprolactone); PCL, poly(caprolactone); PCL-NH_2, aminolyzed PCL.

In vitro cell culture

To explore the improved antiadhesion efficacy offered by the PCL-g-HA NFM in vitro, cell-culture experiments using fibroblasts were performed. Figure 5A shows that the number of viable cells on the PCL NFM was significantly less than that on the PCL-g-HA NFM at days 1 and 7. However, the increase in cell number was not significantly different between the membranes. In a previous report, HA was shown to regulate the proliferation and migration of rabbit tendon fibroblasts.[33,34] Nonetheless, our results suggest that grafted HA only reduces cell attachment but not cell proliferation, which may be beneficial for tendon healing at the site of injury. Since HA has a lubricating effect, the cell adherent was significantly lower on Seprafilm at day 1 than PCL-g-HA NFM. Double-fluorescence staining with the F-actin protein labeled in red and the nucleus counterstained in blue was further used to determine the cytoskeletal arrangement of cells on the membranes (Figure 5B). The morphology of cells attached to the PCL NFM surface was flattened. In comparison, there were fewer cells attached to the PCL-g-HA NFM surface, with a relatively rounded morphology. Taken together, the PCL-g-HA NFM was less prone to cell adhesion and spreading than the PCL NFM. This finding is supported by the results of a previous study in which fibroblasts showed reduced cell adhesion to an HA-containing hydrogel, where cells were also observed to become more rounded in shape with increasing HA concentration and molecular weight.[35] By inhibiting fibroblast attachment, the HA-grafted NFM is expected to synergistically augment the antiadhesion effect of PCL NFMs in vivo.

Table 2 X-ray photoelectron spectroscopy analysis of the surface composition of nanofibrous membranes

Membrane	Atomic percentage			
	C	N	O	Na
PCL	87.80	0	12.20	0
PCL-NH_2	77.89	0.74	21.37	0
PCL-g-HA	74.95	2.68	22.13	0.25

Abbreviations: PCL-g-HA, hyaluronic acid-grafted poly(caprolactone); PCL-NH_2, aminolyzed PCL; PCL, poly(caprolactone).

Table 3 Fraction of the carbon functional groups indicated by high-resolution C_{1s} X-ray photoelectron spectroscopy peaks

Membrane	C–C ~286.6 eV (%)	C–O ~288.1 eV (%)	O=C–O ~290.6 eV (%)	NH–C=O ~289.3 eV (%)
PCL	73.54	19.51	6.95	0
PCL-NH_2	73.31	8.50	10.42	7.77
PCL-g-HA	55.68	21.57	11.55	11.20

Abbreviations: PCL-g-HA, hyaluronic acid-grafted poly(caprolactone); PCL-NH_2, aminolyzed PCL; PCL, poly(caprolactone).

Animal study

Peritendinous adhesion was evaluated at 2 and 8 weeks postoperation by direct gross observation of the repair sites of digits (Figure 6). At both points in time, in the untreated control group, dense adhesion formations were noted around the repaired sites of tendons, which required sharp dissection to separate the large fibrous tissue bundles bridging the surrounding tissue with the tendon.[27] For the case in which Seprafilm and the PCL NFM were used, small bundles of fibrous tissues were observed to loosely bridge the tendon and the surrounding tissue. In contrast, no adhesion was observed for the repaired tendon treated with the PCL-g-HA NFM throughout the experiment.

Figure 7 shows the histological sections of each tendon receiving different treatments in comparison with those of the control group. For the untreated control tendons, severe adhesions occurred between the tendon and the surrounding vascular granulation tissues.[36] Loose bundles of fibrous tissues bridging the repaired tendon and the surrounding tissue can be observed for tendons wrapped with Seprafilm. The surface roughness of a repaired tendon can be used as an indication of the partial healing of the injured tendon. For the case in which PCL NFMs were used, a noticeable interface was only observed at the repaired sites at 2 weeks postoperation, with no significant adhesion formation between repaired tendons and surrounding tissues. Residual fragments of non-degraded NFMs were also observed at the repair interface. Compared with the PCL NFM group, no adhesions between repaired tendons and surrounding tissues were observed for the PCL-g-HA NFM group at both 2 and 8 weeks postoperation. Overall, our objective to use HA grafting to enhance the peritendinous antiadhesion efficacy offered by the PCL NFM was successfully demonstrated in vivo based on gross views and histological assessments; moreover, the enhancement was observed to be better than that offered by a commonly used commercial antiadhesion barrier – Seprafilm. The PCL-g-HA NFM recreated the antiadhesive role of the tendon sheath to prevent tendon adhesion to the surrounding tissue. Previously, Irkören et al reported the successful use of a perichondrium graft to reduce peritendinous adhesion based on macroscopic and histopathological observations.[37] In contrast to the perichondral autograft used in their study, we demonstrated similar antiadhesion effects in this study by using an NFM prepared from a synthetic polymer and grafted with a natural polymer, which did not elicit an inflammatory response around the edges of the barrier (Figure 7).

To assess the in vivo antiadhesion effects of our proposed NFM quantitatively, we conducted a comprehensive range of motion, gliding excursion, and biomechanical evaluation of the FDP tendon. More physiologically and clinically

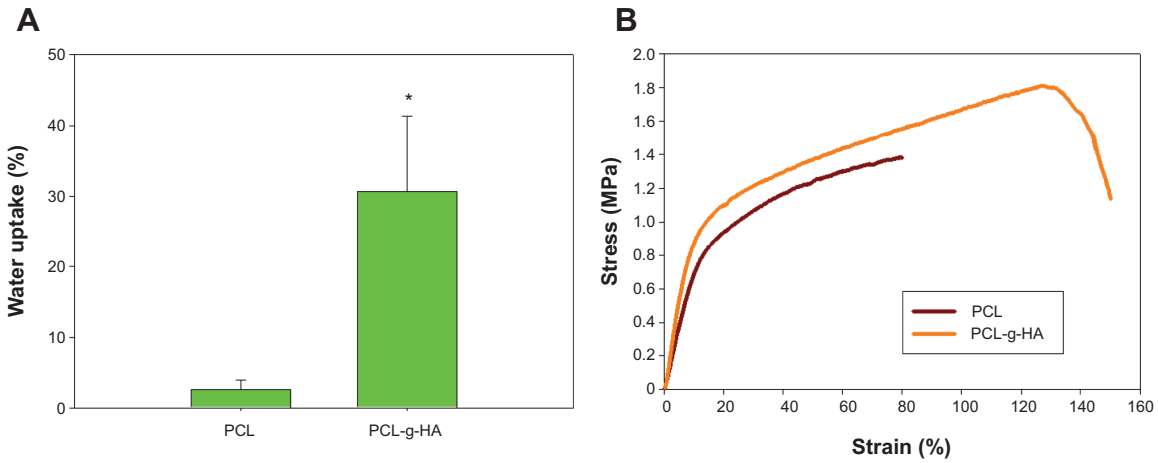

Figure 4 Water sorption (**A**) and representative stress–strain curves (**B**) of PCL and PCL-g-HA nanofibrous membranes.
Note: *$P<0.05$ compared with PCL.
Abbreviations: PCL-g-HA, hyaluronic acid-grafted poly(caprolactone); PCL, poly(caprolactone).

Table 4 Mechanical properties of nanofibrous membranes

Membrane	Ultimate tensile strength (MPa)	Elongation at break (%)	Young's modulus (MPa)
PCL	1.36±0.06	71.75±13.14	7.09±0.19
PCL-g-HA	1.64±0.18*	133.87±33.35*	7.97±1.06

Note: *$P<0.05$ compared with PCL.
Abbreviations: PCL-g-HA, hyaluronic acid-grafted poly(caprolactone); PCL, poly-(caprolactone).

relevant PIP and DIP joint range-of-motion assays were used in the study.[38,39] Compared with the control group, the experimental groups showed a statistical improvement (ie, an increase in value) in DIP joint-flexion angle (Figure 8A), PIP joint-flexion angle (Figure 8B), and sliding excursion (Figure 8C). However, only the PCL-g-HA NFM restored the values to those of the normal unoperated FDP tendons (dotted lines in Figure 8). Peritendinous adhesion was prevented by using different barrier materials but with different improvements over the control. Considering all treatments, tendons treated with NFMs were observed to be better than those treated with Seprafilm, and the efficacy in preventing peritendinous adhesion followed the order of PCL-g-HA NFM > PCL NFM > Seprafilm. At week 8, the DIP and PIP flexion of the PCL-g-HA NFM showed a significant increase over those of the other groups. In addition, at weeks 2 and 8, the gliding excursion of the PCL-g-HA NFM was significantly higher than that of the other groups.

The severity of peritendinous adhesion was assessed based on the pullout force, shown in Figure 8D. The pullout force is the force required to completely remove the tendon from the tendon sheath. The untreated control exhibited

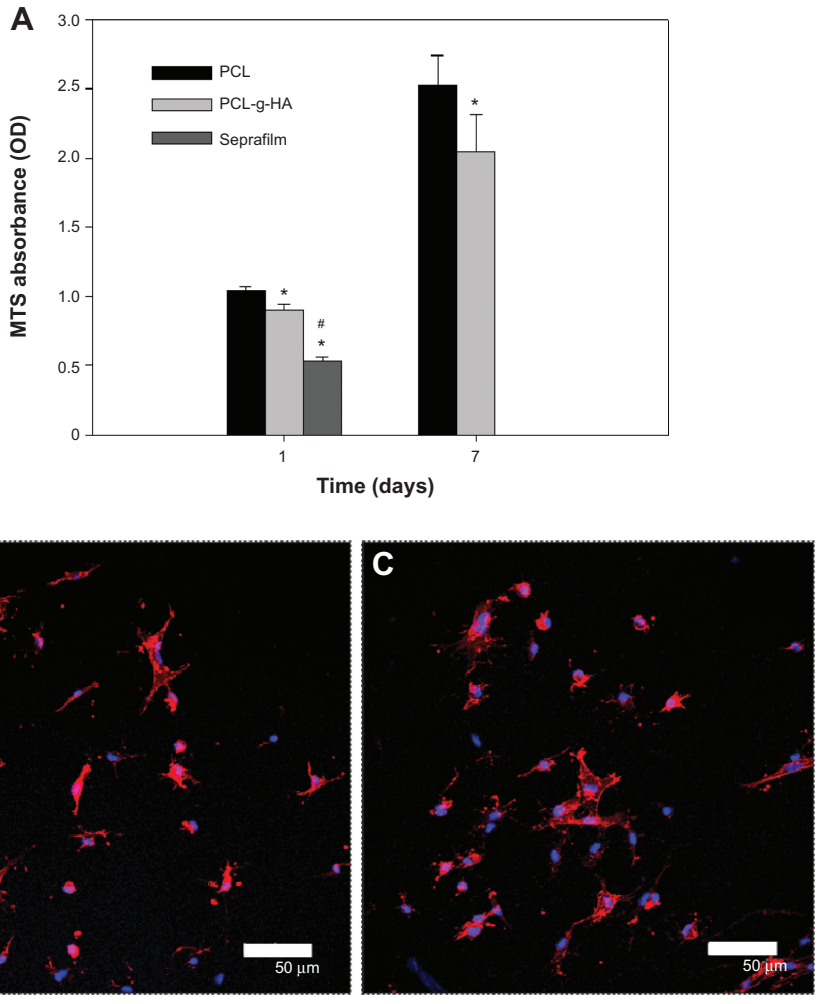

Figure 5 (**A**) Attachment of fibroblasts to PCL and PCL-g-HA nanofibrous membranes and Seprafilm after 1 and 7 days determined by 3-(4,5-dimethylthiazol-2-yl)-5-(3-carboxymethoxyphenyl)-2-(4-sulfophenyl)-2H-tetrazolium assays. The cytoskeletal arrangement of fibroblasts on PCL (**B**) and PCL-g-HA (**C**) nanofibrous membranes was determined by phalloidin/4′,6-diamidino-2-phenylindole staining and observed by confocal microscopy after 24 hours. Bar =50 μm.
Notes: *$P<0.05$ compared with PCL; #$P<0.05$ compared with PCL-g-HA.
Abbreviations: PCL-g-HA, hyaluronic acid-grafted poly(caprolactone); PCL, poly(caprolactone); MTS, 3-(4,5-dimethylthiazol-2-yl)-5-(3-carboxymethoxyphenyl)-2-(4-sulfophenyl)-2H-tetrazolium; OD, optical density.

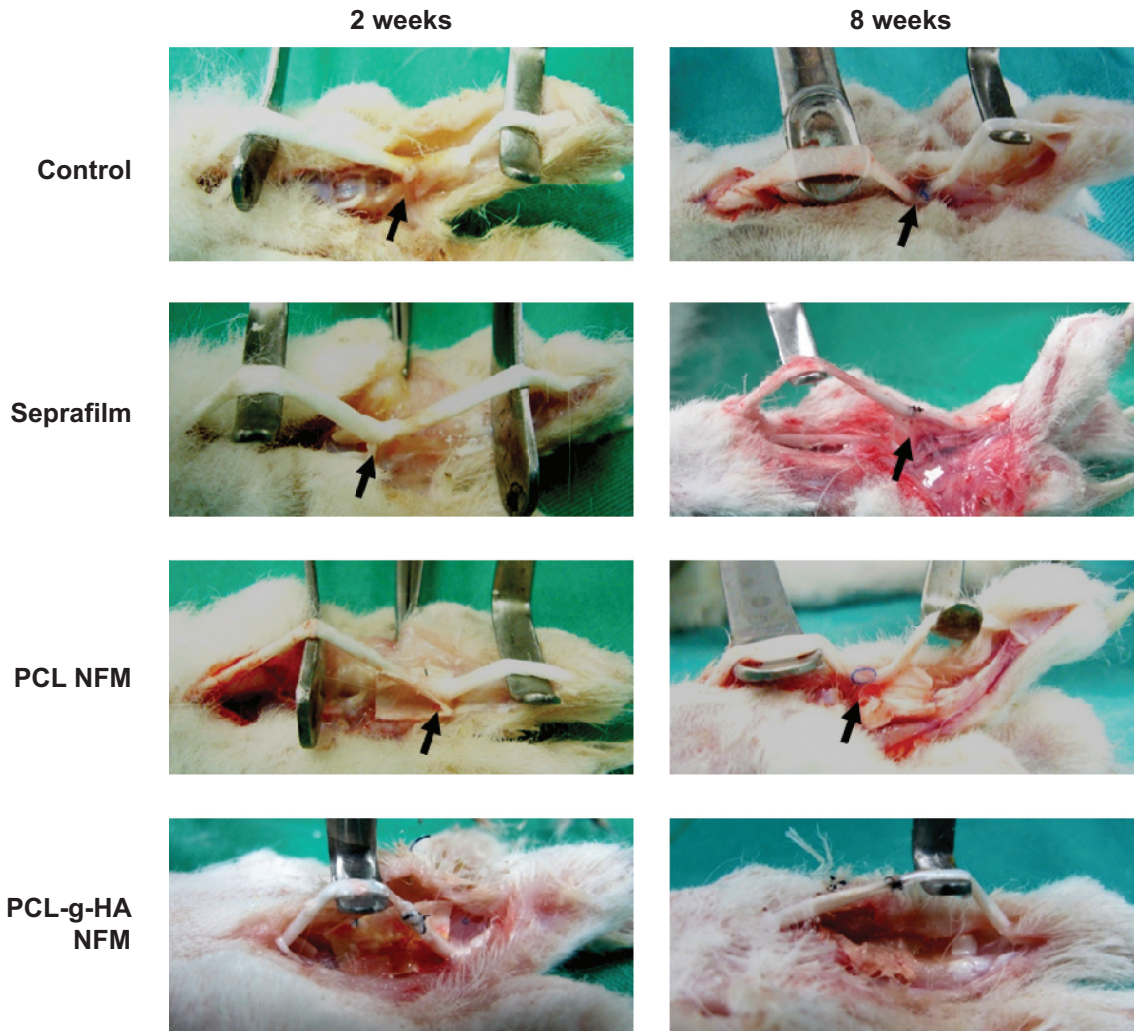

Figure 6 Gross evaluation of adhesion of repaired flexor digitorum profundus tendon in untreated control and repaired tendons wrapped with Seprafilm, PCL, and PCL-g-HA nanofibrous membrane (NFM) at 2 and 8 weeks postoperation. Tendon adhesions (arrows) are indicated in the figures.
Abbreviations: PCL-g-HA, hyaluronic acid-grafted poly(caprolactone); PCL, poly(caprolactone).

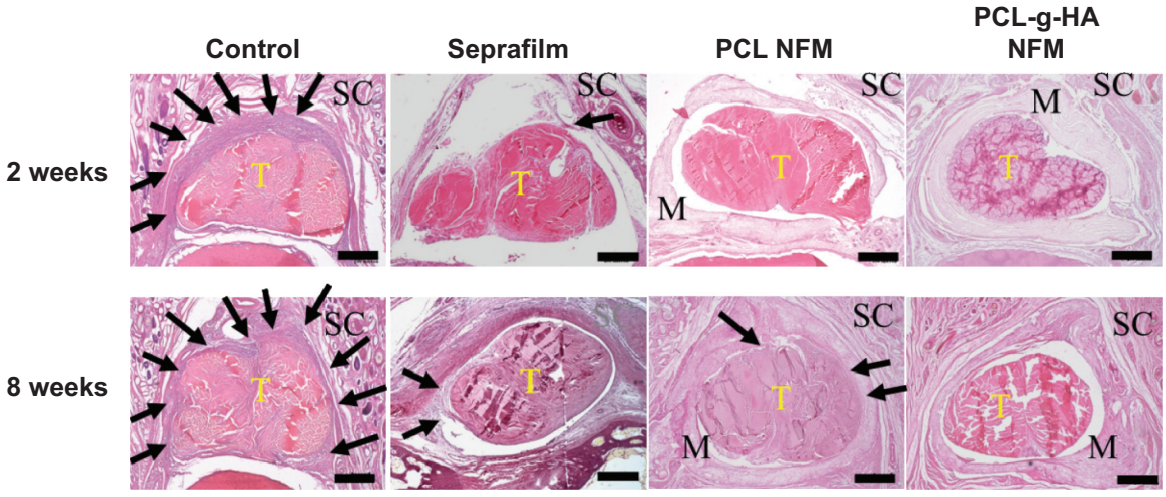

Figure 7 Hematoxylin and eosin staining of tissue sections of the untreated control repair site, repair sites wrapped with Seprafilm, PCL, and PCL-g-HA nanofibrous membrane (NFM) at 2 and 8 weeks postoperation. Arrows indicate adhesion tissues surrounding the tendon. Subcutaneous tissue (SC), tendon (T), and residual membrane (M) were detected. Bar =400 μm.
Abbreviations: PCL-g-HA, hyaluronic acid-grafted poly(caprolactone); PCL, poly(caprolactone).

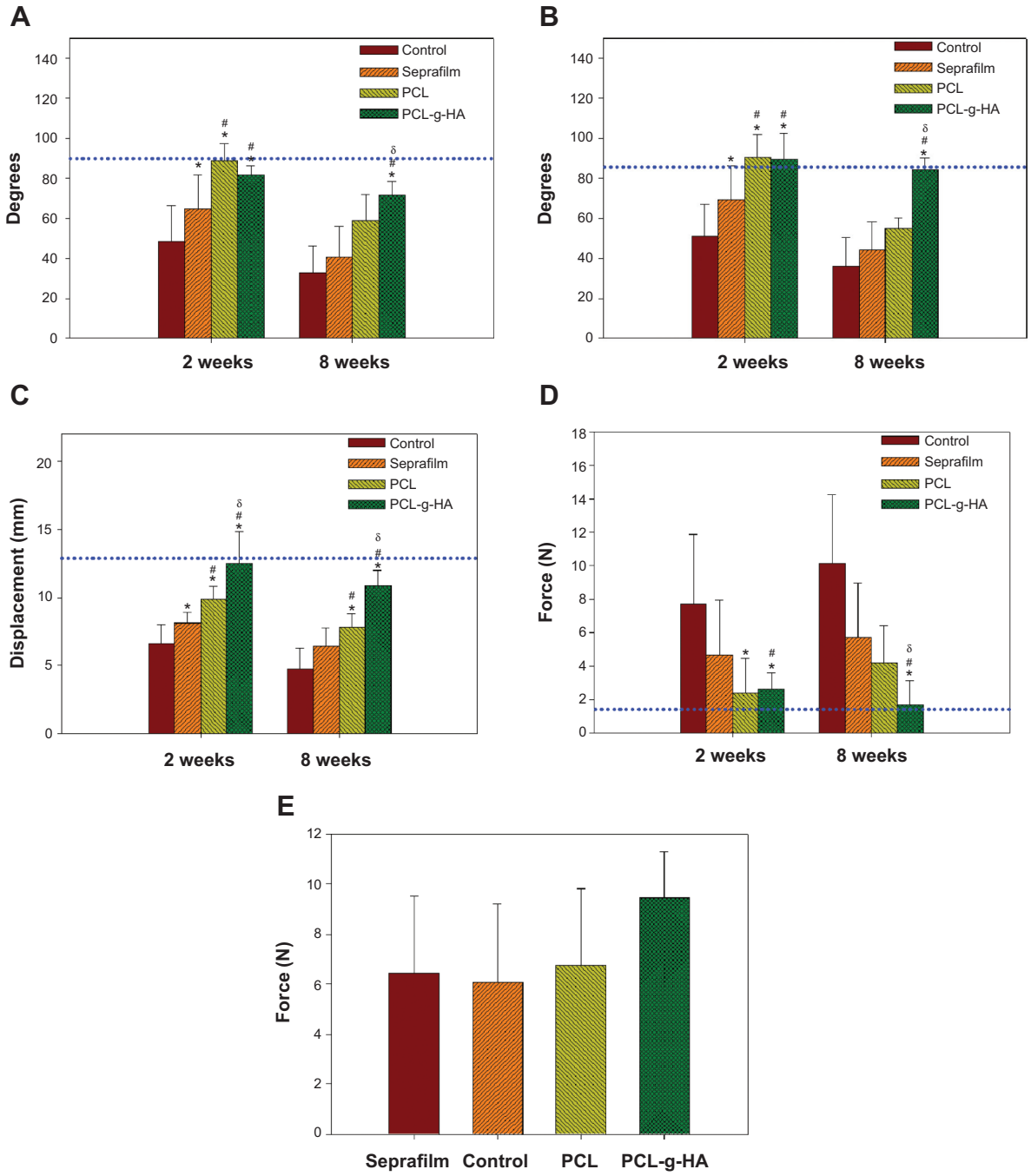

Figure 8 Evaluation of peritendinous adhesions at different times postoperation from distal interphalangeal joint-flexion angle (**A**), proximal interphalangeal joint-flexion angle (**B**), tendon gliding excursion (**C**), pullout force, (**D**) and breaking strength of healed flexor digitorum profundus (FDP) tendons (**E**) at 2 weeks postoperation. The dotted line represents the average value of the initial unoperated FDP tendons.

Notes: *$P<0.05$ compared with untreated control; #$P<0.05$ compared with the group treated with Seprafilm; $^{\delta}P<0.05$ compared with the group treated with PCL nanofibrous membrane. Data are expressed as means ± standard deviation (n=8 for each group).

Abbreviations: PCL-g-HA, hyaluronic acid-grafted poly(caprolactone); PCL, poly(caprolactone).

the maximum value, as expected. Consistent with previous assessments, tendons treated with the PCL-g-HA NFM required the lowest force; the PCL NFM demonstrates an intermediate force, whereas Seprafilm required the largest force. Overall, Seprafilm and the PCL NFM showed limited improvement over the control; the PCL-g-HA NFM significantly lowered the pullout force compared with the pullout forces of all groups at week 8, which was also the only group that could reduce the pullout force to that of a normal unoperated FDP tendon. To study the possible interference of tendon healing by the barrier, the mechanical strength of healed tendons at 2 weeks postoperation

was measured, and is reported in Figure 8E. A distinct increase in the breaking strength of healed tendons was observed for the PCL-g-HA NFM group compared with the breaking strength measured for the other groups. However, the breaking force, which is directly correlated with tendon healing, showed no significant difference among the four groups. We conclude that all antiadhesion barriers had the same healing rate as the untreated control, and most importantly, the NFMs do not obstruct normal tendon healing.[19]

Due to its weak mechanical properties and the relative dimensions of the tendon compared with those of the abdominal cavity, Seprafilm could be a difficult antiadhesion barrier to apply when wrapped around an injured tendon. Moreover, due to the relatively longer healing duration (more than 6 weeks) required after tendon surgery, the fast-degrading nature of Seprafilm cannot offer a residence time that is long enough to allow for adhesion-free healing during the critical first-week period after tendon surgery. The elastic and accessible nature of PCL and PCL-g-HA NFMs allow them to maintain their mechanical integrity during positioning. For the abdominal environment, a soft antiadhesion barrier membrane, such as Seprafilm, may be beneficial to prevent postoperative peritoneal adhesion. However, because the tendon-tissue surface will experience frequent gliding motion, a good adhesion barrier like Seprafilm that suits the needs of a tissue surface with limited motion may not be a good option for peritendinous applications. From this perspective, the PCL-g-HA NFM is expected to provide better mechanical strength and an improved ability to isolate a moving tendon from the surrounding tissue during the healing phase to prevent peritendinous adhesion.

Conclusion

Electrospun PCL and PCL-g-HA NFMs were successfully prepared to prevent peritendinous adhesion and to serve as biomimetic tendon sheaths. Surface grafting of HA to a PCL NFM enhances the water sorption and the mechanical strength of the NFM while maintaining the fiber diameter and its microporous structure. In vitro studies revealed that the HA-grafted PCL NFM reduced fibroblast attachment without impeding cell proliferation. In vivo studies using a rabbit FDP tendon model demonstrated the advantage of the PCL-g-HA NFM in preventing peritendinous adhesion over the PCL NFM and a commonly used commercial antiadhesion barrier (Seprafilm), based on biomechanical, histological, and functional analyses.

Acknowledgments

Financial support from the National Science Council (NSC102-2320-B-182-004-MY3), the Department of Health (DOH102-TD-PB-111-NSC004), and Chang Gung Memorial Hospital (CMRPG3A1431-2) is gratefully appreciated.

Disclosure

The authors report no conflicts of interest in this work.

References

1. Liakakos T, Thomakos N, Fine PM, Dervenis C, Young RL. Peritoneal adhesions: etiology, pathophysiology, and clinical significance. Recent advances in prevention and management. *Dig Surg*. 2001;18:260–273.
2. Taras JS, Lamb MJ. Treatment of flexor tendon injuries: surgeons' perspective. *J Hand Ther*. 1999;12:141–148.
3. Lilly SI, Messer TM. Complications after treatment of flexor tendon injuries. *J Am Acad Orthop Surg*. 2006;14:387–396.
4. Boyer MI. Flexor tendon biology. *Hand Clin*. 2005;21:159–166.
5. Yeo Y, Kohane DS. Polymers in the prevention of peritoneal adhesions. *Eur J Pharm Biopharm*. 2008;68:57–66.
6. diZerega GS, Campeau JD. Peritoneal repair and post-surgical adhesion formation. *Hum Reprod Update*. 2001;7:547–555.
7. Hagberg L, Heinegard D, Ohlsson K. The contents of macromolecule solutes in flexor tendon sheath fluid and their relation to synovial fluid. A quantitative analysis. *J Hand Surg Br*. 1992;17:167–171.
8. Peterson WW, Manske PR, Dunlap J, Horwitz DS, Kahn B. Effect of various methods of restoring flexor sheath integrity on the formation of adhesions after tendon injury. *J Hand Surg Am*. 1990;15:48–56.
9. Bolgen N, Vargel I, Korkusuz P, Menceloğlu YZ, Pişkin E. In vivo performance of antibiotic embedded electrospun PCL membranes for prevention of abdominal adhesions. *J Biomed Mater Res B Appl Biomater*. 2007;81:530–543.
10. Wu Q, Li L, Wang N, et al. Biodegradable and thermosensitive micelles inhibit ischemia-induced postoperative peritoneal adhesion. *Int J Nanomedicine*. 2014;9:727–734.
11. Akasaka T, Nishida J, Araki S, Shimamura T, Amadio PC, An KN. Hyaluronic acid diminishes the resistance to excursion after flexor tendon repair: an in vitro biomechanical study. *J Biomech*. 2005;38:503–507.
12. Zhao C, Sun YL, Kirk RL, et al. Effects of a lubricin-containing compound on the results of flexor tendon repair in a canine model in vivo. *J Bone Joint Surg Am*. 2010;92:1453–1461.
13. Isık S, Öztürk S, Gürses S, et al. Prevention of restrictive adhesions in primary tendon repair by HA-membrane: experimental research in chickens. *Br J Plast Surg*. 1999;52:373–379.
14. Huang ZM, Zhang YZ, Kotaki M, Ramakrishna S. A review on polymer nanofibers by electrospinning and their applications in nanocomposites. *Compos Sci Technol*. 2003;63:2223–2253.
15. Chang JJ, Lee YH, Wu MH, Yang MC, Chien CT. Electrospun antiadhesion barrier made of chitosan alginate for reducing peritoneal adhesions. *Carbohydr Polym*. 2012;88:1304–1312.
16. Dinarvand P, Hashemi SM, Seyedjafari E, et al. Function of poly(lactic-co-glycolic acid) nanofiber in reduction of adhesion bands. *J Surg Res*. 2012;172:e1–e9.
17. Yang DJ, Chen F, Xiong ZC, Xiong CD, Wang YZ. Tissue anti-adhesion potential of biodegradable PELA electrospun membranes. *Acta Biomater*. 2009;5:2467–2474.
18. Zong X, Li S, Chen E, et al. Prevention of postsurgery-induced abdominal adhesions by electrospun bioabsorbable nanofibrous poly(lactide-co-glycolide)-based membranes. *Ann Surg*. 2004;240:910–915.

19. Liu S, Zhao J, Ruan H, et al. Biomimetic sheath membrane via electrospinning for antiadhesion of repaired tendon. *Biomacromolecules*. 2012;13:3611–3619.
20. Liu S, Hu C, Li F, Li XJ, Cui W, Fan C. Prevention of peritendinous adhesions with electrospun ibuprofen-loaded poly(L-lactic acid)-polyethylene glycol fibrous membranes. *Tissue Eng Part A*. 2013;19:529–537.
21. Ma Z, He W, Yong T, Ramakrishna S. Grafting of gelatin on electrospun poly(caprolactone) nanofibers to improve endothelial cell spreading and proliferation and to control cell orientation. *Tissue Eng*. 2005;11:1149–1158.
22. Du F, Zhao W, Zhang M, Mao H, Kong D, Yang J. The synergistic effect of aligned nanofibers and hyaluronic acid modification on endothelial cell behavior for vascular tissue engineering. *J Nanosci Nanotechnol*. 2011;11:6718–6725.
23. Mattanavee W, Suwantong O, Puthong S, Bunaprasert T, Hoven VP, Supaphol P. Immobilization of biomolecules on the surface of electrospun polycaprolactone fibrous scaffolds for tissue engineering. *ACS Appl Mater Interfaces*. 2009;1:1076–1085.
24. Zhu Y, Gao C, Liu X, Shen J. Surface modification of polycaprolactone membrane via aminolysis and biomacromolecule immobilization for promoting cytocompatibility of human endothelial cells. *Biomacromolecules*. 2002;3:1312–1319.
25. Chen JP, Chen SH, Lai GJ. Preparation and characterization of biomimetic silk fibroin/chitosan composite nanofibers by electrospinning for osteoblasts culture. *Nanoscale Res Lett*. 2012;7:170.
26. Ishiyama N, Moro T, Ohe T, et al. Reduction of peritendinous adhesions by hydrogel containing biocompatible phospholipid polymer MPC for tendon repair. *J Bone Joint Surg Am*. 2011;93:142–149.
27. Liu Y, Skardal A, Shu XZ, Prestwich GD. Prevention of peritendinous adhesions using a hyaluronan-derived hydrogel film following partial-thickness flexor tendon injury. *J Orthop Res*. 2008;26:562–569.
28. Karakurum G, Buyukbebeci O, Kalender M, Gulec A. Seprafilm interposition for preventing adhesion formation after tenolysis. An experimental study on the chicken flexor tendons. *J Surg Res*. 2003;113:195–200.
29. Chen JP, Cheng TH. Preparation and evaluation of thermo-reversible copolymer hydrogels containing chitosan and hyaluronic acid as injectable cell carriers. *Polymer*. 2009;50:107–116.
30. Chen JP, Chang YS. Preparation and characterization of composite nanofibers of polycaprolactone and nanohydroxyapatite for osteogenic differentiation of mesenchymal stem cells. *Colloids Surf B Biointerfaces*. 2011;86:169–175.
31. Chen JP, Su CH. Surface modification of electrospun PLLA nanofibers by plasma treatment and cationized gelatin immobilization for cartilage tissue engineering. *Acta Biomater*. 2011;7:234–243.
32. Bölgen N, Menceloğlu YZ, Acatay K, Vargel I, Pişkin E. In vitro and in vivo degradation of non-woven materials made of poly(caprolactone) nanofibers prepared by electrospinning under different conditions. *J Biomater Sci Polym Ed*. 2005;16:1537–1555.
33. Wiig M, Abrahamsson SO, Lundborg G. Effects of hyaluronan on cell proliferation and collagen synthesis: a study of rabbit flexor tendons in vitro. *J Hand Surg Am*. 1996;21:599–604.
34. Yagi M, Sato N, Mitsui Y, Gotoh M, Hamada T, Nagata K. Hyaluronan modulates proliferation and migration of rabbit fibroblasts derived from flexor tendon epitenon and endotenon. *J Hand Surg*. 2010;35:791–796.
35. Ouasti S, Donno R, Cellesi F, Sherratt MJ, Terenghi G, Tirelli N. Network connectivity, mechanical properties and cell adhesion for hyaluronic acid/PEG hydrogels. *Biomaterials*. 2011;32:6456–6470.
36. Xu L, Cao D, Liu W, Zhou G, Zhang WJ, Cao Y. In vivo engineering of a functional tendon sheath in a hen model. *Biomaterials*. 2010;31:3894–3902.
37. Irkören S, Demirdöver C, Akad BZ, Aytuğ Z, Yilmaz E, Oztan Y. Use of a perichondrial autograft on the peritendinous adhesion: an experimental study in rabbits. *Acta Orthop Traumatol Turc*. 2012;46:208–214.
38. Chang J, Thunder R, Most D, Longaker MT, Lineaweaver WC. Studies in flexor tendon wound healing: neutralizing antibody to TGF-β1 increases postoperative range of motion. *Plast Reconstr Surg*. 2000;105:148–155.
39. Namba J, Shimada K, Saito M, Murase T, Yamada H, Yoshikawa H. Modulation of peritendinous adhesion formation by alginate solution in a rabbit flexor tendon model. *J Biomed Mater Res B Appl Biomater*. 2007;80:273–279.